Modelocking of a Frequency Shifted Feedback Laser triggered by Amplitude Modulation

MIGUEL CUENCA[1], HAROLDO MAESTRE[1], AND CARLOS R. FERNÁNDEZ-POUSA[1,*]

[1] *Engineering Research Institute I3E, Universidad Miguel Hernández, Av. Universidad s/n, E03202 Elche, Spain*
[*] *c.pousa@umh.es*

Compiled January 24, 2024

We report an experimental technique to trigger modelocking (ML) emission in Frequency-Shifted Feedback (FSF) lasers. These lasers feature an intracavity modulator driven by a radio-frequency tone, which shifts the light spectrum every cavity roundtrip. The technique consists of the drive of the modulator with a second tone at the cavity free spectral range (FSR) frequency. So, in addition to the frequency shift, a weak amplitude modulation (AM) appears synchronous with the cavity roundtrip time. The approach is successful as FSF cavities support chirped modes evenly spaced by the FSR, whose AM coupling produces convenient seed pulses for the ML onset. This results in ML emission at arbitrary frequency shifts and initiation thresholds lower than in standard, spontaneous FSF laser ML. Simulations indicate that the role of AM is to trigger the formation of ML pulses, but the primary mechanism of pulse buildup is Kerr effect. The technique opens a new practical route to initiate ML emission in FSF lasers.

http://dx.doi.org/10.1364/ao.XX.XXXXXX

The generation of optical pulses with tunable wavelengths represents a recurrent demand from different fields, such as spectroscopy, chemical, biological, and optical sensing, and line-of-sight communications. The incorporation of an acousto-optic frequency-shifting device in a laser cavity is one of the conceptually most simple means for the generation of this type of emission. With increasing pump power, these so-called Frequency-Shifted Feedback (FSF) lasers spontaneously emit pulses with a repetition rate equal to the free spectral range (FSR) of the cavity, and so they are usually understood as a particular type of modelocked (ML) lasers. In addition, acousto-optic ML FSF lasers offer access to different emission bands due to the wide spectral transparency of acousto-optic materials. Over the years, acousto-optic ML FSF lasers with pulse widths in the ps to sub-ps range have been demonstrated in different cavity configurations and active media, including lasers in the visible range (DCM dye [1], Ti:sapphire [2]) and silica-based doped fiber lasers in the near infrared (Er [3], Nd [4], Er/Yb [5], Yb [6], Tm [7]). More recently, and due to its self-starting nature, they are receiving renewed attention in the development of fluoride glass pulsed fiber lasers for the mid infrared band (Dy:ZBLAN [8], Ho/Pr:ZBLAN [9], Er:ZrF_4 [10]), as a compact alternative to other, more conventional, ML techniques.

Despite this number of demonstrations, the development of ML FSF lasers still poses some challenges of both practical and conceptual nature. On the practical side, they may present relatively large emission thresholds, as the ML regime typically shows up within a hysteresis cycle [1, 2, 7]. On the conceptual side, its theoretical description dwells on the early work by Sabert and Brinkmeyer [4] who first recognized the role of Kerr effect in pulse buildup. Self-phase modulation (SPM) broadens the spectrum of the recirculating waves and therefore counteracts the unidirectional spectral displacement induced by the frequency shift. Consequently, a stable phase distribution across the spectrum can be attained, eventually resulting in pulses. Using the master equation of modelocking, Martjin de Sterke and Steel [11] showed that ML emission in FSF lasers arises from the combination of gain, filtering, Kerr effect, and frequency shift, and results in asymmetric and nonlinearly chirped pulses. Nonetheless, this general framework, which has been confirmed in simulations [5, 8, 12] and direct measurements [13], does not refer to any modal representation or locking mechanism among recirculating waves, and so it is not unusual to find judicious caveats about the pertinence of referring to this emission regime as modelocked [8–10].

In this Letter, we address these issues and show that, owing to the structure of the recirculating modes, it is possible to trigger the initiation of ML emission by inducing a coupling of modes through amplitude modulation (AM) in a manner similar to that in active ML. Our study is based on an Er:fiber ring FSF laser incorporating a fiber-coupled acousto-optic frequency shifter (AOFS), extends preliminary demonstrations of the technique [14, 15], and unveils the origin of certain related dynamical effects reported in [9, 16]. Specifically, we demonstrate fundamental ML induction by engineering the radio-frequency (RF) waveform driving the AOFS, which is modulated in amplitude at a rate equal to the FSR, and show that this process results in a reduction in the ML emission threshold. The technique requires no additional intracavity hardware, is applicable, in principle, to any emission band, and can be even the result of an unintentional, residual modulation originated in the AOFS.

Let us consider the electric field $E(t)$ that recirculates in an ideal, lossless, and dispersion-free ring cavity incorporating a frequency shifter. After a roundtrip, the electric field transforms into $E'(t) = e^{-i2\pi f_s t}E(t-\tau_c)$, where τ_c is the roundtrip time and

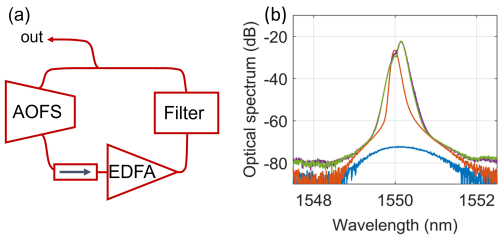

Fig. 1. (a) Scheme of a FSF laser. (b) Optical spectrum of the FSF laser in different regimes: blue, below threshold; orange, CW emission above threshold; green, self-starting ML emission; and magenta, AM-triggered ML emission.

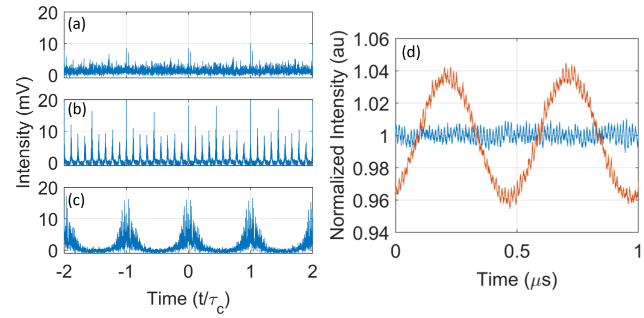

Fig. 2. Intensity of the CW regime of the FSF laser at (a) f_s = 80 MHz, (b) f_s = 81.785 MHz ($f_s\tau_c = 9$), and (c) f_s = 80 MHz with AM modulation ($\mu = 0.005$). (d) Intensity recorded after the AOFS when driven by a f_s = 80 MHz tone (blue) and by the same tone with an additional AM modulation with $\mu = 0.02$ and modulation frequency of 2 MHz (orange).

f_s the shifting frequency. Modes, understood as fields invariant under this roundtrip transformation, are waves chirped at a rate f_s/τ_c and evenly spaced in frequency with respect to the FSR $= 1/\tau_c$ [17]. The resulting modal expansion is:

$$E(t) = e^{-i\pi \frac{f_s}{\tau_c} t^2 - i\pi f_s t} \sum_k A_k e^{-i2\pi k \frac{t}{\tau_c}} \tag{1}$$

where A_k are arbitrary complex amplitudes. This expansion also represents the basis of the so-called moving comb model of the CW regime of FSF lasers, where the laser is operated above threshold and the emission due to amplified ASE recirculation [18–21]. In this regard, it was originally pointed out in [18] that a coupling between the amplitudes A_k in (1) may eventually result in pulses. A direct consequence of this observation, which seems to have remained unexplored, is that one could use a suitable, intentional temporal modulation to trigger the process of ML pulse generation. An additional motivation of this approach follows from the analysis of the ML onset in our laser, which we describe next.

Our FSF laser, previously described in [16] and schematically shown in Fig. 1(a), comprises a fiber loop (length ∼22 m, FSR = 9.087 MHz) including an EDFA (length 60 cm) followed by a fiber Bragg grating of center wavelength 1550 nm and FWHM of 1.63 nm acting as an intracavity bandlimiting filter. An AOFS provides positive frequency shifts in the range 73-83 MHz and an isolator assures unidirectional recirculation. The EDFA was operated at a fixed gain of 17 dB and cavity losses were controlled through the RF power driving the AOFS. When the cavity is below threshold, the laser emits ASE with a spectrum determined by the FBG spectral reflectivity, as shown in the blue trace of Fig. 1(b). Just above threshold, ASE recirculation results in CW emission with a spectral peak shifted from the FBG center in the direction of the frequency shift, as shown by the orange trace in that figure. With decreasing losses, the laser becomes Q-switched (QS) by self-sustained relaxation oscillations in the amplifier [16, 22]. Finally, when the laser is operated with a gain ∼2 dB above loss, the laser spontaneously emits ML pulses but only in the so-called integer or semi-integer resonant conditions. These conditions are defined by a frequency shift tuned to a harmonic or subharmonic of the FSR and so verifying $f_s\tau_c = p/q$ with p and q coprime integers. The ML spectrum is centered near the FBG peak and shows a shoulder at the peak of CW emission, as can be observed in the green trace of Fig. 1(b).

In [16] we observed that, at resonant conditions, ML emission is preceded by the appearance of pulse-like ASE recirculation patterns in both CW and QS regimes and from which the ML pulses evolve. In Fig. 2, we present the CW intensity corresponding to (a) f_s = 80 MHz and (b) the integer resonance $f_s\tau_c = 9$. In the first of these plots the intensity appears as a quasiperiodic stream of recirculating ASE spikes with a period equal to the roundtrip time. In turn, in Fig. 2(b) this recirculation is organized in pulses whose origin, which could not be identified in [16], is the existence of a residual modulation in the AOFS that synchronously reinforces in each roundtrip. To show this, the AOFS was isolated, fed by a polarized laser line at 1550 nm, and its intensity detected by a low-noise, amplified photodiode. Under different input states of polarization the intensity presented a small, and variable in depth, modulation in amplitude at the driving frequency f_s. A representative example corresponding to an input polarization optimized for minimum AOFS loss is depicted in blue in Fig. 2(d). This modulation stems from the interference in the AOFS output of the first order beam, which is frequency shifted, with the zeroth order beam, which is unshifted and partially overlapping with the output port [23]. The existence of an unidentified modulation of this type when the frequency shift is adjusted to the resonant condition f_s = FSR was first reported in [9] to lead to high-purity ML in a Ho/Pr:ZBLAN FSF laser. Thus, the mechanism of ML induction in [9, 16] can be described as follows: the residual AM induces a coupling among the chirped modes in Eq. (1) that results in a periodic, pulse-like ASE recirculation pattern, from which ML pulses build up through SPM due to the local enhancement of Kerr effect. Hence, an intentional AM at a modulation frequency equal to the FSR, superimposed to an arbitrary frequency shift f_s, is expected to trigger the ML emission in the same way.

Following these observations, we addressed the AOFS with an electrical waveform $V(t) = V_0\,[1 + \mu\cos(2\pi t/\tau_c)]\cos(2\pi f_s t)$ comprising a carrier at the desired frequency shift f_s modulated in amplitude at a modulation frequency fine tuned to the cavity's FSR, $\mu < 1$ being the electrical modulation index. When fed with an optical wave at frequency ν_0, the AOFS thus creates three frequency shifted waves, the first with frequency $\nu_0 + f_s$ and two small sidebands at $\nu_0 + f_s \pm$ FSR. The amplitudes of the optical modulation sidebands are proportional to μ, and the optical modulation index μ_o observed in the intensity is ideally the double of μ. Limitations in AOFS bandwidth decrease the conversion to $\mu_o \simeq 1.2\mu$ when the modulation frequency equals the FSR. A sample trace of the the observed optical intensity after impressing the AM with a modulation frequency of 2 MHz is shown in orange in Fig. 2(d).

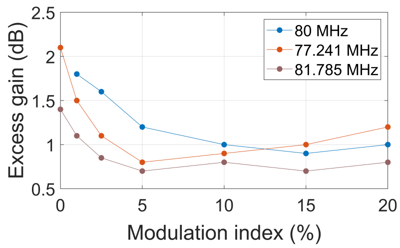

Fig. 3. Excess gain for the observed ML threshold, in dB, at different shifting frequencies f_s and electrical modulation indices μ. Zero modulation index refers to a situation where the AOFS is driven by a single RF tone without AM, for which ML induction at $f_s = 80$ MHz was not possible in our laser.

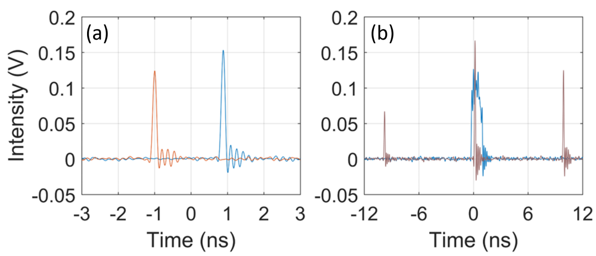

Fig. 4. (a) Pulse intensity in self-starting ML emission at the integer resonant condition (orange) and AM-triggered ML at $f_s = 80$ MHz (blue). (b) Pulse cluster (blue) generated by AM-triggered ML and its drift (brown) when the AM is turned off.

In Fig. 2(c) we depict the output intensity just above threshold with the AOFS fed with the AM driving waveform, showing the expected recirculation in the form of ASE bursts at a repetition rate equal to the FSR. With decreasing losses, we could observe ML emission for arbitrary values of the frequency shift, even out of resonant conditions where we were previously unsuccessful. We characterized the excess gain of the ML onset, measured as dB above threshold, for different values of the shifting frequency by the following procedure. For each modulation index μ, the cavity was first driven below threshold by decreasing the RF power delivered to the AOFS. The threshold RF power was determined by the observation in the optical spectrum of the strong CW peak exemplified in Fig. 1(b). The cavity loss was further decreased by increasing the RF power until reaching the ML regime. RF power is finally transferred to optical dB by use of a calibration table. The results, plotted in Fig. 3, show a decrease down to $\sim$1 dB in all cases where we incorporate AM, with small variations with respect to the imparted frequency shift. Moreover, at low modulation indices we observed that, once the ML regime is attained, the AM can be switched off and the laser remains in the ML state. In turn, with high modulation indices, typically above 5%, the laser returns to CW or QS when the AM is deactivated, a fact that we ascribe to the accompanying destabilization of the laser dynamics. Recalling that the self-starting ML regime of these lasers typically shows hysteresis, these observations suggest that the present technique induces underlying ML states that, without AM, can only be reached through the decreasing path of the hysteresis cycle.

After turning the AM off, we did not observe any fundamental difference between the ML emission generated with and without AM. In Fig. 1(b), the spectrum is similar for both cases, with (magenta) and without AM (green). The pulse intensity in Fig. 4(a), recorded with a high-speed (50 GHz) photodiode and a digital oscilloscope of 6 GHz bandwidth, also appears similar, with a ringing in the pulse's trailing edge due to bandwidth-limited detection. The RF intensity spectrum also shows the same features both with and without AM [14]. The only difference we observed appeared when the AM is switched off at high relative pump levels. In this case, the ML emission of FSF lasers, as is typical in fiber lasers, shows up as a cluster of pulses [4, 7, 13, 16] which drift apart and occupy equispaced positions, thus leading to a form of harmonic ML. Under the action of AM, however, the cluster remains packed as exemplified by the blue trace in Fig. 4(b). The drift only starts when the AM is turned off, as shown by the brown trace in that figure.

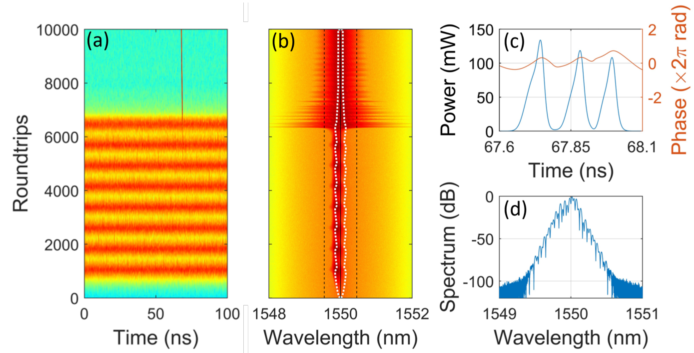

Fig. 5. Intensity (a) and spectral (b) maps of the self-starting ML regime induced by Kerr effect (see **Visualization 1**). (c) Pulse intensity and phase and (d) optical spectrum at the final recirculation. In (b), the dashed lines represent the filter's FWHM and the white dotted trace the frequencies where the filter is at threshold.

The preceding results indicate that the incorporation of AM favors the ML onset, but the primary role in the pulse buildup process is to be ascribed to Kerr effect. To provide further support to this view, we performed a series of simulations using a single-polarization recirculation map of the intracavity field $E_n(t)$ that introduces, in this order, gain G_n and filtering, SPM, frequency shift, modulation, and loss $T < 1$, according to:

$$E_n(t) \rightarrow E_{n+1}(t) = \sqrt{T}\left[1 + \mu\cos(2\pi t/\tau_c)\right] e^{-i2\pi f_s t} \cdot e^{i\gamma L_{\text{eff}}\left(G_n|\widetilde{E}_n(t)|^2 + |\widetilde{E}_s(t)|^2\right)} \cdot \left[\sqrt{G_n}\widetilde{E}_n(t) + \widetilde{E}_s(t)\right] \quad \textbf{(2)}$$

Here, n is the recirculation index, L_{eff} is the effective nonlinear length, γ is the Kerr coefficient (1.2 $\text{W}^{-1}\text{km}^{-1}$ in standard fiber), and $\widetilde{E}_n(t) = \mathcal{F}^{-1}\left[H(\omega)\mathcal{F}(E_n(t))\right]$ is the filter's output, with $H(\omega)$ the filter's spectral amplitude response, here assumed gaussian and centered at 1550 nm, and $\mathcal{F}$ the Fourier transform operator. Gain dynamics is accounted for by a standard saturation equation defined by its low-signal (unsaturated) gain (17 dB), saturation power (12 mW) and gain recovery time (540 µs), figures that were extracted from our EDFA in separate experiments. The model is seeded by a field $\widetilde{E}_s(t)$ that describes the filtered ASE generated in the amplifier. ASE is introduced in the spectral domain as a gaussian process with spectral density $S_{\text{ASE}} = n_{\text{sp}} h\nu_0 (G - 1)$, where $n_{\text{sp}} = 1.7$, h is the Planck's constant and ν_0 the frequency corresponding to 1550 nm. This ASE level is updated in each roundtrip according to the saturated gain G_n. Loop dispersion was not initially considered.

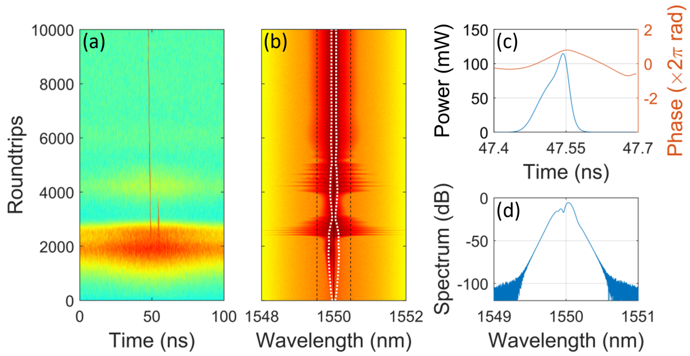

Fig. 6. Same as in Fig. 5 but with a loss of 16 dB and triggered by AM ($\mu = 0.005$) during the first 5000 recirculations. The final pulse width is 58 ps (FWHM). See **Visualization 2**.

In a first example, we simulated the self-starting ML regime induced by Kerr effect, without AM. Mimicking our system, the filter's width was 115 GHz (FWHM) and the total loss 15 dB, with f_s=80 MHz and τ_c=100 ns. L_{eff} was estimated to be 12 m. The results are contained in Fig. 5. Focusing first in the spectral map of Fig. 5(b) and in analogy with our experiment, the laser reaches ML from a QS regime observable for $n \lesssim 6000$. This QS regime is characterized by a spectrum that accumulates on the edge of the portion of the filter lying above threshold, in the direction of the frequency shift, and follows a standard gain depletion-recovery process [16, 22]. During depletion, the spectral range where the cavity is above threshold, shown with a dotted white trace, narrows but does not totally close; gain recovers and another QS pulse builds up. In the temporal map of Fig. 5(a) QS pulses are observed as bands representing constant light levels over each roundtrip that are smoothly switched on and off. A ML pulse or a cluster of ML pulses are created from ASE spikes during gain saturation; they show up as sudden phase distributions across the optical spectrum concentrated in the filter's peak, as observed as a series of wide, narrow bands in the spectral map after $n \sim 6000$. These pulses pick up all the gain offered by the amplifier in its recovery, increase its spectral width through SPM, and override the ASE that builds the QS pulses. For this process to take place, it is critical that a portion of the filter remains above threshold during gain depletion, otherwise the laser stays in a robust QS regime. After the generation of the ML pulses, gain stabilizes, sometimes by erasing some pulses from the cluster, and the ML emission sets in the form of a series of surviving pulses, in this case three as depicted in Fig. 5(c). The spectrum shown in Fig. 5(d) presents interference due to the mutual coherence among the pulses in the cluster.

In the second simulation of Fig. 6 the loop loss was increased up to 16 dB and an AM with $\mu = 0.005$ was activated during the first 5000 roundtrips. At this loss level, the simulation does not reach the ML regime without AM. Here, the laser evolves towards ML at $n \sim 2500$ from an initial recovery of the gain after erasing some transient pulses. The general description of the process is however similar, and again relies on the spectral broadening offered by Kerr effect to an ASE spike. In the temporal domain, AM provides a low-loss temporal window where ASE can grow and build the ML pulse. After turning the AM off at recirculation 5000, the ML emission remains. The final state comprises a single asymmetric and nonlinearly chirped pulse of the type described in [11].

Both simulations also show the existence of a drift in the ML pulse position with respect to the cold cavity's roundtrip time, a drift that is more pronounced with the introduction of loop's dispersion in the simulations. This points that, while the introduction of AM is beneficial for initiating ML, maintaining AM after ML induction may become detrimental in the long term, as it would induce a modulation in the pulse train due to the mismatch between pulses' repetition rate and FSR. In fact, in our experiment we were able to observe ML emission with maintained AM and with a fundamental RF tone free of spurious only after a readjustment of the AM modulation frequency.

In conclusion, we have reported a practical technique for triggering ML emission by introducing AM in the frequency shifting element of acousto-optic FSF lasers. The AM lowers the pump threshold of ML and broadens the useful frequency-shift range to apparently arbitrary values. The technique can be straightforwardly applied to existing FSF lasers as it does not require additional elements. Conceptually, our results support the view that ML emission in FSF lasers can be understood as a process of locking of chirped modes.

Funding. Agencia Estatal de Investigación (PID2020-120404GB-I00, EQC2019-006189-P); Ministerio de Universidades (FPU21/05449).

Acknowledgments. The authors thank fruitful discussions with Germán J. de Valcárcel and Germán Torregrosa.

Disclosures. The authors declare no conflicts of interest.

Data availability. Data underlying the results presented in this paper are not publicly available at this time but may be obtained from the authors upon reasonable request.

REFERENCES

1. S. Balle and K. Bergmann, Opt. Commun. **116**, 136 (1995).
2. G. Bonnet, S. Balle, Th. Kraft, and K. Bergmann, Opt. Commun. **123**, 790 (1996).
3. P. Myslinski, J. Chrostowski, J. A. K. Koningstein, and J. R. Simpson, Appl. Opt. **32**, 286 (1993).
4. H. Sabert and E. Brinkmeyer, J. Lightw. Technol. **12**, 1360 (1994).
5. S. H. Yun, D. J. Richardson, D. O. Culverhouse, and B. Y. Kim, IEEE J. Sel. Top. Quantum Electron. **3**, 1087 (1997).
6. J. Porta *et al.*, Opt. Lett. **23**, 615 (1998).
7. H. Chen, S.-P. Che, Z.-F. Jiang, and J. Hou, Sci. Rep. **6**, 26431 (2016).
8. R. I. Woodward, M. R. Majewski, and S. D. Jackson, APL Photonics **3**, 116106 (2018).
9. M. R. Majewski, R. I. Woodward, and S. D. Jackson, Opt. Lett. **44**, 1698 (2019).
10. O. Henderson-Sapir *et al.*, Opt. Lett. **45**, 224 (2020).
11. C. Martjin de Sterke and M. J. Steel, Opt. Commun. **117**, 469 (1995).
12. L. A. Vazquez-Zuniga and Y. Jeong, Opt. Commun. **322**, 54 (2014).
13. Z. Gao and T. Mei, Opt. Lett. **47**, 4973 (2022).
14. M. Cuenca, H. Maestre, G. Torregrosa, and C. R. Fernández-Pousa, in *Frontiers in Optics + Laser Science 2023* (FIO, LS), Technical Digest Series (Optica Publishing Group, 2023), paper JTu5A.68.
15. J. Lecourt *et al.*, in *Conference on Lasers and Electro-Optics/Europe* (CLEO/Europe 2023), Technical Digest Series (Optica Publishing Group, 2023), paper cj_3_6.
16. M. Cuenca *et al.*, Opt. Express **31**, 15615 (2023).
17. W. Streifer and J. R. Whinnery, Appl. Phys. Lett. **17**, 335 (1970).
18. S. Balle, I. C. Littler, K. Bergmann, and F. V. Kowalski, Opt. Commun. **102**, 166 (1993).
19. K. Nakamura *et al.*, IEEE J. Quantum Electron. **33**, 103 (1997).
20. L. P. Yatsenko, B. W. Shore, and K. Bergmann, Opt. Commun. **236**, 183 (2004).
21. H. Guillet de Chatellus *et al.*, Opt. Commun. **284**, 4965 (2011).
22. J.-N. Maran, P. Besnard, and S. LaRochelle, J. Opt. Soc. Am. B **23**, 1302 (2006).
23. F. Darde, *AA Opto-Electronic*, private communication.

REFERENCES

1. S. Balle and K. Bergmann, "Self-pulsing and instabilities in a unidirectional ring dye laser with intracavity frequency shift," Opt. Commun. **116**(1-3), 136-142 (1995).
2. G. Bonnet, S. Balle, Th. Kraft, and K. Bergmann, "Dynamics and self-modelocking of a titanium-sapphire laser with intracavity frequency-shifted feedback," Opt. Commun. **123**(4-6), 790-800 (1996).
3. P. Myslinski, J. Chrostowski, J. A. K. Koningstein, and J. R. Simpson, "Self-mode locking in a Q-switched erbium-doped fiber laser," Appl. Opt. **32**(3), 286-290 (1993).
4. H. Sabert and E. Brinkmeyer, "Pulse generation in fiber lasers with frequency shifted feedback," J. Lightw. Technol. **12**(8), 1360-1368 (1994).
5. S. H. Yun, D. J. Richardson, D. O. Culverhouse, and B. Y. Kim, "Wavelength-swept fiber laser with frequency shifted feedback and resonantly swept intra-cavity acoustooptic tunable filter," IEEE J. Sel. Top. Quantum Electron. **3**(4), 1087-1096 (1997).
6. J. Porta, A. B. Grudinin, Z. J. Chen, J. D. Minelly, and N. J. Traynor, "Environmentally stable picosecond ytterbium fiber laser with a broad tuning range," Opt. Lett. **23**(8), 615-617 (1998).
7. H. Chen, S.-P. Che, Z.-F. Jiang, and J. Hou, "Diversified pulse generation from frequency shifted feedback Tm-doped fibre lasers," Sci. Rep. **6**, 26431 (2016).
8. R. I. Woodward, M. R. Majewski, and S. D. Jackson,"Mode-locked dysprosium fiber laser: Picosecond pulse generation from 2.97 to 3.30 μm," APL Photonics **3**(11), 116106 (2018).
9. M. R. Majewski, R. I. Woodward, and S. D. Jackson, "Ultrafast mid-infrared fiber laser mode-locked using frequency-shifted feedback," Opt. Lett. **44**(7), 1698-1701 (2019).
10. O. Henderson-Sapir, N. Bawden, M. R. Majewski, R. I. Woodward, D. J. Ottaway, and S. D. Jackson, "Mode-locked and tunable fiber laser at the 3.5 μm band using frequency-shifted feedback," Opt. Lett. **45**(1), 224-227 (2020).
11. C. Martjin de Sterke and M. J. Steel, "Simple model for pulse formation in laser with a frequency-shifting element and nonlinearity," Opt. Commun. **117**(5-6), 469-474 (1995).
12. L. A. Vazquez-Zuniga and Y. Jeong, "Study of a mode-locked erbium-doped frequency-shifted-feedback fiber laser incorporating a broad bandpass filter: Numerical results," Opt. Commun. **322**, 54-60 (2014).
13. Z. Gao and T. Mei, "Spectro-temporal evolution of mode-locked lasing in fiber frequency-shifted feedback laser," Opt. Lett. **47**(19), 4973-4976 (2022).
14. M. Cuenca, H. Maestre, G. Torregrosa, and C. R. Fernández-Pousa, "Locking of chirped modes using amplitude modulation in acousto-optic frequency shifted feedback fiber lasers," in *Frontiers in Optics + Laser Science 2023* (FIO, LS), Technical Digest Series (Optica Publishing Group, 2023), paper JTu5A.68.
15. J. Lecourt *et al.*, "Frequency-Shifted-Feedback Mode-Locked Fibre Laser with Tuneable Repetition Rate," in *Conference on Lasers and Electro-Optics/Europe* (CLEO/Europe 2023), Technical Digest Series (Optica Publishing Group, 2023), paper cj_3_6.
16. M. Cuenca, H. Maestre, G. Torregrosa, H. Guillet de Chatellus, and C. R. Fernández-Pousa, "ASE recirculation effects in pulsed frequency shifted feedback lasers at large frequency shifts," Opt. Express **31**(10), 15615-15636 (2023).
17. W. Streifer and J. R. Whinnery, "Analysis of a dye laser tuned by acousto-optic filter," Appl. Phys. Lett. **17**(8), 335-337 (1970).
18. S. Balle, I. C. Littler, K. Bergmann, and F. V. Kowalski, "Frequency shifted feedback dye laser operating at a small shift frequency," Opt. Commun. **102**(1-2), 166-174 (1993).
19. K. Nakamura, F. Abe, K. Kasahara, T. Hara, M. Sato, and H. Ito, "Spectral characteristics of an all solid-state frequency-shifted feedback laser," IEEE J. Quantum Electron. **33**(1), 103-111 (1997).
20. L. P. Yatsenko, B. W. Shore, and K. Bergmann, "Theory of a frequency-shifted feedback laser," Opt. Commun. **236**(1-3), 183-202 (2004).
21. H. Guillet de Chatellus, E. Lacot, W. Glastre, O. Jacquin, and O. Hugon, "The hypothesis of the moving comb in frequency shifted feedback lasers," Opt. Commun. **284**(20), 4965-4970 (2011).
22. J.-N. Maran, P. Besnard, and S. LaRochelle, "Theoretical analysis of a pulsed regime observed with a frequency-shifted-feedback fiber laser," J. Opt. Soc. Am. B **23**(7), 1302-1311 (2006).
23. F. Darde, *AA Opto-Electronic*, private communication.